# DESIGN OF CODED TARGETS AND AUTOMATED MEASUREMENT PROCEDURES IN INDUSTRIAL VISION METROLOGY

**Susumu Hattori, Keiichi Akimoto*, Clive Fraser** Tetsu Ono*** and Harutaka Imoto******

Fukuyama University, Japan, Dept. of Computer Science
hattori@fuip.fukuyama-u.ac.jp
*Shikoku Polytechnic College, Japan, Dept. of Control Engineering,
akimoto@kagawa-pc.ac.jp
** University of Melbourne, Australia, Dept. of Geomatics
c.fraser@eng.unimelb.adu.au
*** Kyoto University, Japan, Dept. of Global Engineering
ono@jf.gee.kyoto-u.ac.jp
**** Ishikawajima-Harima Heavy Industries Co.,Ltd., Japan, Dept. of Production Engineering
harutaka_imoto@ihi.co.jp

Working Group V/1

**KEY WORDS:** Industrial vision metrology, CCD cameras, Coded targets, Exterior orientation devices, Closed-form similarity transformation.

## ABSTRACT

In industrial photogrammetric measurement with CCD cameras, the number of target images may amount to several hundred when large and complex objects are involved. It is therefore impractical to use solely manual means to identify these image points. This paper reports on a further design for coded targets, which can be automatically located and identified, and it also discusses special arrangements of reference targets called exterior orientation devices. These can be employed in conjunction with new computational schemes for sensor orientation to facilitate automated data processing. Procedures adopted to ensure sufficient speed and reliability in automated off-line digital photogrammetric measurements employing these developments, which have been found in practise to reduce data processing time by as much as 93%, are discussed and experimental results are reported.

## 1 INTRODUCTION

Off-line industrial photogrammetric measurement with CCD cameras typically utilises retroreflective targets to signalise feature points, which are recorded in multiple images. This targetting approach has long been adopted, for reasons of both cost and precision, for large and complex objects such as ship sections and bridge blocks (Fraser, 1993; Fraser et al.,1998). With increasing object size and an emphasis on surface contour determination, the number of required target points can become very large, with several hundred being not at all uncommon for curved ship blocks. Coupled with the fact that between 30 and 100 images might be used within the photogrammetric network, this can add significantly to the burden of photogrammetric measurement if manual identification is relied upon in the data processing phase, which will involve thousands of image point measurements. As a further complication to manual identification processes, retro-reflective targets generally appear as simple dots on a significantly underexposed background.

Prior to bundle adjustment, approximations of all the parameters (interior and exterior orientation parameters, and object coordinates) are necessary. Once again, manual involvement in this determination of preliminary parameter values is quite undesirable from a productivity point of view, and also from a reliability standpoint given that labelling errors are to be expected in underexposed imagery with dense target fields. In order to overcome these problems, developments in measurement automation based on coded targets (CTs) and exterior orientation (EO) devices have been carried out (eg Fraser, 1997; Ganci & Handley, 1998; Hattori et al., 1999).

In the present paper, the authors present a process for automated off-line vision metrology which employs CTs, an EO device for initiating sensor orientation, and a computational scheme which uses a closed-form 3D similarity transformation algorithm for preliminary EO. The scheme also employs a strategy of sequential image connection

followed by determination of image point correspondences for uncoded targets and a final bundle adjustment phase. An experimental application of the process, which has proven to be fast, robust and reliable, is then discussed.

## 2 FLOW OF MEASUREMENT PROCEDURE

In general, coded targets are too large to be employed for all objects points (Niederoest & Maas, 1996, Fraser, 1997), and indeed there is no need to consider such a course of action since CTs are primarily used for initial EO determination, often in conjunction with EO devices. Moreover, they need only be imaged from selected camera stations, preferably more than three, whereas standard retro-reflective targets for measurement (MTs) are placed at all interest points on the object. One procedure that can be adopted for measurement based on the use of CTs is as follows:

(a) For efficient measurement, prior plans of camera and target configurations are considered and tested with a CAD simulator, though this phase is often dispensed with.

(b) Following image recording, all CTs in all images are recognised and identified to check the connectivity of images.

(c) The imaging network is altered through image addition (or subtraction) if the degree of connectivity is not sufficient.

(d) The images are connected one by one for coarse, preliminary orientation, thus yielding an approximate EO for bundle adjustment.

(e) Bundle adjustment is performed to obtain an initial refinement of EO parameters and XYZ coordinates of CTs, after which MTs are iteratively identified and their object space coordinates estimated by multi-ray intersection.

(f) A bundle adjustment is performed to compute the final parameter values for the multi-image measurement network.

## 3 CODED TARGET DESIGN

To date, there have been two main types of CTs developed, concentric rings (van den Heuvel et al.,1992; Niederoest & Maas, 1996) and dot distributions (Ganci & Handley,1998). The former feature a relatively limited number of code possibilities, but display simple and stable recognition and decoding performance (Hattori et al., 1999). The latter require a more complex identification algorithm, but allow for a greater number of code numbers/labels. The design discussed here, which produces 420 code numbers, belongs to the dot distribution group.

The developed CT, as shown in Figs.1and 2, consists of six retro-reflective circular dots, three of which define the origin and the coordinate axes, while the pattern of the rest represents the code. The size of the code arrangement will depend on imaging scale and the dimensions shown in Fig. 1 are appropriate for the experimental testing reported in Sect. 7, which involved a relatively large imaging scale of around 1:50. The size of each reflective circular dot is the same as that for the adopted MT shown in Fig.3. An image of the CT is deformed by affine projection, for example to the shape indicated in Fig.2, when viewed from an oblique incidence angle. In the set of 420 possible codes, a one-to-one correspondence is maintained in deformed patterns of three points under affine transformation.

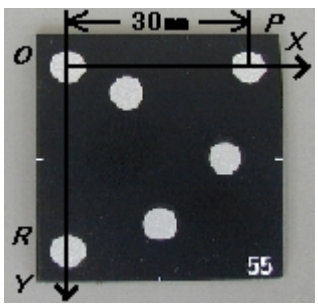


Figure 1. Coded target.

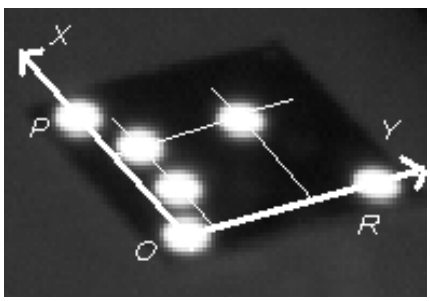


Figure 2. Affine-distorted image of a CT.

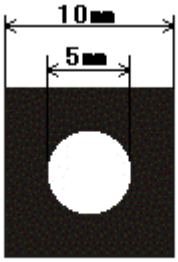


Figure 3. Codeless MT.

The reading process for the CT proceeds as follows:

- An image is first binarized by adaptive threshold values and then the blobs forming the code are extracted by an image dilation technique. If six reflective targets merge to one segment, the group is regarded as a CT.

- Three dots (image blobs), P, O and R, which define the code xy coordinate axes, are searched for. Emerging patterns of CT images are sorted into appearance order for this purpose. Dark and small images of CTs are rejected as undeterminable, and every combination of axis candidates from a CT image is then compared to a model pattern. Candidates of points P, O and R are tested by projecting the remaining three dots to the axes (see Fig.2) and ascertaining whether they fall within a parallelogram defined by P, O and R. The ID number of the code is also uniquely determined at this time.

## 4 CONNECTION AND ESTIMATION OF EXTERIOR ORIENTATION PARAMETERS

In the proposed strategy for the use of CTs to support automated measurement, alternative network configuration plans warrant comparison in regard to the disposition of CTs and MTs, as well as with respect to camera station geometry and other photogrammetric design factors. This 'network simulation' is quite effective in measurement planning for complex objects because the first-order design (Fraser, 1984) also allows the image connections, and therefore suitable CT distributions, to be established. Taking into account that a significant percentage of large manufactured components nowadays have an associated design model in CAD, the authors have developed a network simulator, indicated in Fig. 4, which works in conjunction with an off-the-shelf CAD system.

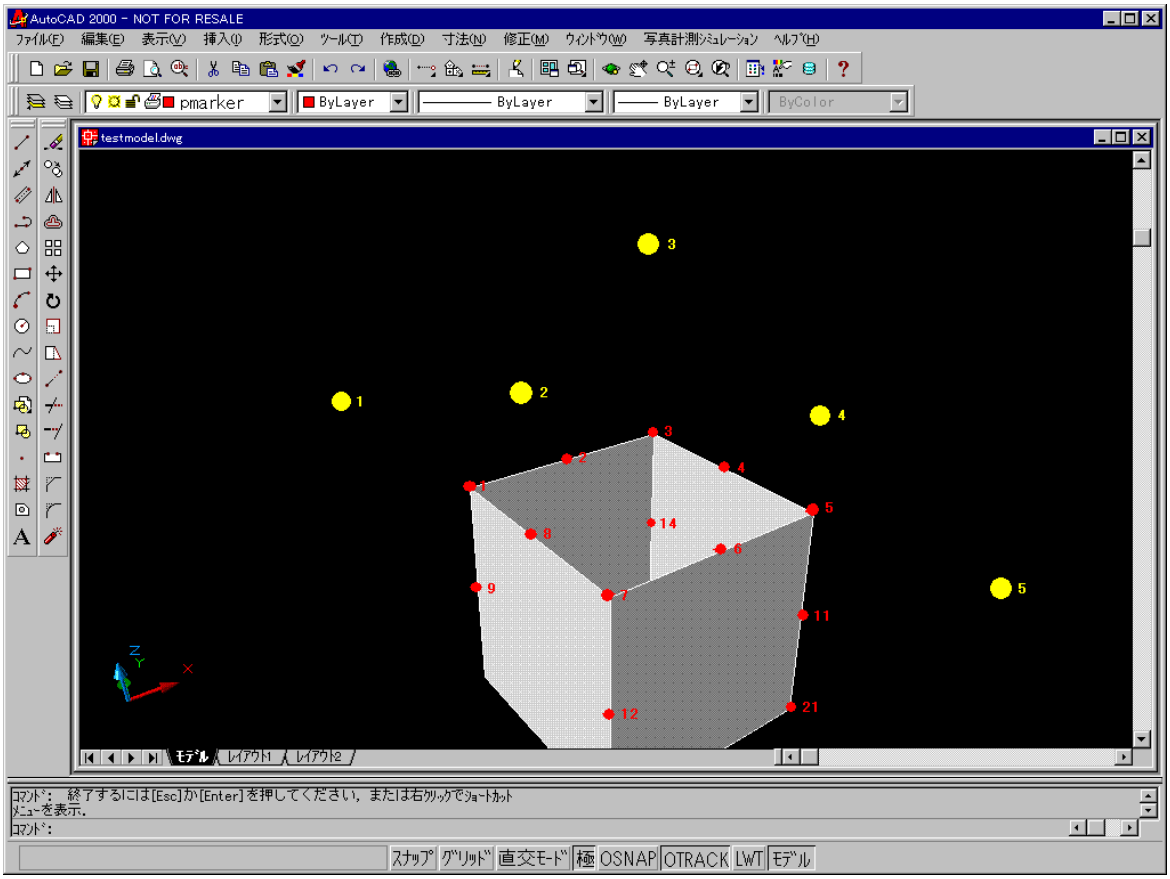


Figure 4. Screen display of the CAD integrated network simulator.

By means of the simulator it can be checked that all proposed images will include at least three well-recognisable CTs. Camera station positions need only be approximated to support this operation. Where there is a deficiency in CT distribution, either extra images are added or additional CTs are utilised, as appropriate. It is of course always possible to use some MTs in the role of CTs, but the assignment of labels must be manual in this case. These MTs could, for example, be definition points for a desired reference coordinate system, or even control points on a scale bar.

The image connection process proceeds sequentially, with images being successively connected to a chosen first image pair. The initial two (and possibly more) images are oriented by referring to the specially designed EO device, the reference cross shown in Fig. 5. This is a portable 2D target array comprising six retro-reflective dots whose

coordinates are known accurately in a device-specific 3D coordinate system. The absolute scale of the EO device is not critical; indeed very robust sensor orientation can be obtained with relatively small target separation. The dimensions shown in Fig. 5 are once again appropriate to the object used in the reported experiment. The initial two images are so taken that the EO device lies near the frame centers. The approximate orientation of the two initial images is obtained by a direct linear transformation (DLT), after which a bundle adjustment is carried out using all available CTs. The resulting eleven parameters of the DLT are converted to six EO parameters, while the estimated internal orientation parameters are disregarded.

The third and ensuing images are approximately oriented by single image orientation using three or more CTs whose object space coordinates have already been estimated. Though other alternatives for this 'resection' can be employed, a closed-form of the 3D similarity transformation, which is discussed in the following section, has proven to be a very fast and robust approach, which has produced optimal performance in the experiments conducted to date. Other possible approaches include those based on a conventional collinearity model, or on the DLT.

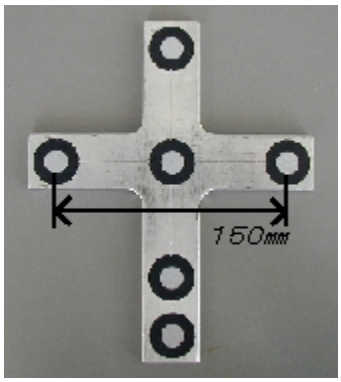


Figure 5. Reference cross EO device.

With the addition of each new image in the sequential network connection process, the object space coordinates of newly available CTs are first estimated by intersection and then refined by a bundle adjustment 'update'.

The order in which the images are connected is an important factor for efficient processing under the proposed process. It is not always practical to take images in the pre-planned connection sequence for complex-shaped objects, but it is important to treat the images in an order which ensures continuity in the propagation of the known XYZ reference system to newly added CTs. It is always feasible after image capture to determine the best connection order, considering the distribution of CTs within the images. Once all the images are connected and oriented approximately, all system parameters are updated by bundle adjustment in order to support efficient correspondence determination of MTs.

## 5 CLOSED FORM OF SIMILARITY TRANSFORMATION

By comparing the lengths, PO and RO in Fig.2 with design values, the scale of a CT image, s, is calculated. Since CT images are small, parallel projection from object space to image space is assumed for this calculation. Let the camera station coordinates be $(X_0,Y_0,Z_0)$ , then

$$\begin{bmatrix} x_i & y_i & -c \end{bmatrix}^T = s_i M \begin{bmatrix} X_i - X_0 & Y_i - Y_0 & Z_i - Z_0 \end{bmatrix}^T \text{ or } \boldsymbol{x_i} = s_i M \left( \boldsymbol{X_i} - \boldsymbol{X_0} \right) \qquad (1)$$

where $\boldsymbol{x_i} = \begin{bmatrix} x_i & y_i & -c \end{bmatrix}^T$ are object coordinates of image point *i*, *c* is the camera distance, *s* a scale factor, *M* a rotation matrix and $\boldsymbol{X_i} = \begin{bmatrix} X_i & Y_i & Z_i \end{bmatrix}^T$ are corresponding object space coordinates with an origin at $\boldsymbol{X_0} = \begin{bmatrix} X_0 & Y_0 & Z_0 \end{bmatrix}^T$ . By normalizing image coordinates by scales,

$$\boldsymbol{u_i} = M \left( \boldsymbol{X_i} - \boldsymbol{X_0} \right) \qquad (2)$$

is obtained, where $\boldsymbol{u} = \begin{bmatrix} x & y & -c \end{bmatrix}^T / s$. Let $\boldsymbol{X_G} = \begin{pmatrix} X_G & Y_G & Z_G \end{pmatrix}^T$ be a gravity center of the object space and $\boldsymbol{u_g}$ be a gravity center of the normalized image coordinates. Then

$$\boldsymbol{u_i} - \boldsymbol{u_g} = M\left(\boldsymbol{X_i} - \boldsymbol{X_G}\right) \text{ or } \overline{\boldsymbol{u}}_i = M\overline{\boldsymbol{X}}_i \tag{3}$$

The rotation matrix M is estimated so as to minimize the square sum of discrepancies of Eq.3;

$$v^2 = \left(\overline{\boldsymbol{u}}_i - M\overline{\boldsymbol{X}}_i\right)^T\left(\overline{\boldsymbol{u}}_i - M\overline{\boldsymbol{X}}_i\right) = - \left(\overline{\boldsymbol{X}}_i^{\,T} M^T \overline{\boldsymbol{u}}_i\right) + const. \rightarrow \min \tag{4}$$

Eq.4 reaches the minimum, when

$$\left(\overline{\boldsymbol{X}}_i^{\,T} M^T \overline{\boldsymbol{u}}_i\right) = trace\left(\overline{\boldsymbol{u}}_i \overline{\boldsymbol{X}}_i^{\,T} M^T\right) \tag{5}$$

reaches the maximum. Singular-value-decomposition of the correlation matrix $C = \overline{\boldsymbol{u}}_i \overline{\boldsymbol{X}}_i^{\,T}$ leads to

$$\overline{\boldsymbol{u}}_i \overline{\boldsymbol{X}}_i^{\,T} = V^T \Lambda W \tag{6}$$

where *V, W* are orthogonal matrices and $\Lambda$ is a diagonal matrix with elements of positive singular values in ascending order. The optimal M that minimizes Eq.5 is given by

$$M = V^T W \tag{7}$$

The camera station coordinates are finally given by, referring to eq.2:

$$\boldsymbol{X_0} = \boldsymbol{X_G} - M^T \boldsymbol{u_g} \tag{8}$$

## 6 IDENTIFICATION OF MTs

Once all the images are connected and a unified network is formed, all uncoded MTs are identified by multi-ray intersection from neighbouring images. To eliminate improbable candidate image points for intersection, only MTs included in image groups which share common CTs are examined. As a threshold value for the multi-ray intersection, a multiple of the root mean square (RMS) value of the standard errors of camera station coordinates is employed, whereas final gross error detection is performed within the subsequent bundle adjustment which includes CTs and MTs.
This bundle adjustment is executed by free-network adjustment with a Moore-Penrose generalized inverse and it is thus referred to neither the coordinate datum of the reference cross, nor a designated object space reference system. Instead, the datum is implicitly assigned within the process of minimizing the mean variance of all parameters. The rank deficiency in observation equations is compensated by adding seven basis vectors in the complement of the null space (Akimoto et al., 1998).

The identification process for MTs is iterative. The first iteration identifies non-ambiguous targets only, and the remainder are kept for later processing. Orientation parameters are then updated. The second and further iterations are employed to identify the remaining targets, until no further improvement is achieved. Operator intervention and checking are allowed at every stage. The overall final bundle triangulation with all validated MTs is executed again by a free-network adjustment, but this time with the constraint of minimal mean variance for the object space coordinates of MTs only, the result of which determines the precision of the triangulated object points.

## 7 EXPERIMENT

In order to evaluate the performance of the CT approach integrated with the new computational scheme, a number of experimental measurements were conducted. One of these is summarized here to exemplify the results obtained. The test object was the iron box (600 x 400 x 300mm) shown in Fig.6. On the five faces of the sides and top, 144 MTs and

29 CTs were placed, along with the EO device. For metric verification, object space coordinates of MTs were measured with a five-axis NC machine (Mitsui Precision Machinery model HS5A) to an estimated measurement precision of 0.01mm. The camera used was a 'stabilised' Kodak DCS460 B/W (3K x 2K pixel array) with a Nikon 20mm lens.

Figure 6. Test box showing EO device, CTs and MTs.

Fig.7 illustrates the exposure station configuration, which comprises 34 camera stations including two nadir-looking and eight from different elevations. This network geometry inevitably arose because the object was placed on a table.

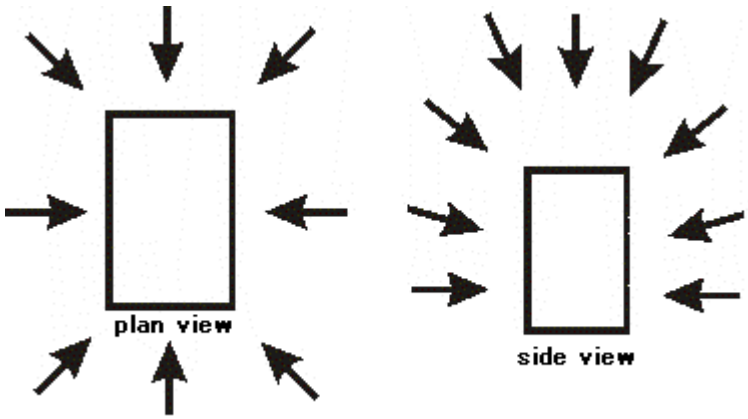


Figure 7. Camera station configuration.

Images were recorded with a range of orthogonal camera roll angles and the camera-to-object distance was set so as to image the box such that it filled the frame format. The task of image capture consumed only about 15 minutes. In the resulting 34-station network there were 2,015 target images, including 213 images of CTs. Four to eight well recognizable CTs were found in every image, and all were correctly identified with the adopted decoding algorithm.

Of the MT images, 76% were identified in the first spatial intersection, which followed the bundle adjustment utilising only CTs. Five of these, all near the extremeties of the image format, were correctly located gross measurement errors. Within the second intersection iteration, 99% of all MTs had been accounted for, though a small number required manual intervention to correct wrong labelling. The total data processing time (ie excluding camera operation and ruling out some minor manual tasks) was four minutes.

For comparison, a full manual measurement operation was carried out, including identification of MTs and input of approximations of exterior orientation parameters. This took 60 minutes, which means the new computational process with CTs saved 93% of work time. As regards measurement accuracy, the RMS discrepancy value between the coordinates measured by vision metrology and those measured by NC machine was 0.04mm (1/25 pixels).

## 8 CONCLUDING REMARKS

In order to enhance vision metrology performance, an automated image measurement and data processing scheme has been developed, which utilises CTs, EO devices, an alternative algorithm for preliminary sensor orientation and a process for sequential image connection via CTs to form the network for bundle triangulation. Determination of image point correspondences of targets through spatial intersection is also accommodated, and the single image orientation has been based on a closed-form similarity transformation, a method needing only three CTs in each image to ensure connectivity. The computational process has been illustrated through the measurement of an iron box, and the performance has been compared against manual operation. Results show the developed method to be very encouraging for practical implementation in vision metrology systems.

## REFERENCES

Akimoto, K., Fraser, C., Hasegawa H. & S. Hattori, 1998. Comparison of free network solutions by the artificial basis-based method with one by the generalized inverse in video metrology, IAPRS, Hokodate, 32 (5): 17-22.

Fraser, C., 1984. Network design consideration for non-topographic photogrammetry, PE&RS, 50 (8): 1115-1126.

Fraser, C., 1993. A Resume of some industrial applications of photogrammetry, ISPRS Journal of Photogramm. & Rem. Sens., 48 (3): 12-23.

Fraser, C., 1997. Innovations in automation for vision metrology systems. Photogramm. Rec., 15 (90): 901-911.

Fraser, C., Hattori, S., Akimoto, K. & N. Uno, 1998. Vision-based dimensional inspection of freeway bridge blocks, IAPRS, Hakodate, 32 (5): 47-52.

Ganci, G & H. Handley, 1998. Automation in videogrammetry, IAPRS, Hakodate, 32(5): 53-58.

Hattori, S., Akimoto, K., Okamoto, A., Hasegawa, H. & C. Fraser, 1999. The design and use of coded targets for automatic measurement with a CCD camera, Proc. ASPRS Annual Convention, Portland, May 17-21, pp. 928-935.

van den Heuvel, F., Kroon, R. & R. le Poole, 1992. Digital close-range photogrammetry using artificial targets. IAPRS, 29 (B5): 222-229

Niederoest, M. & H.-G. Maas, 1996. Entwurf und Erkennung von codierten Zeilmarken, Jahrestagung der Deutschen Gesellschaft fuer Photogrammetrie und Fernerkundung, Oldenburg, Sept. 18-20, 6 pages.